Confinement of steel buckling by concrete in composite members

Autor(en): **Sakai, Masami / Chida, Nobuhiko / Nasu, Toshio**

Objekttyp: **Article**

Zeitschrift: **IABSE reports = Rapports AIPC = IVBH Berichte**

Band (Jahr): **48 (1985)**

PDF erstellt am: **19.05.2024**

Persistenter Link: https://doi.org/10.5169/seals-37476

Confinement of Steel Buckling by Concrete in Composite Members

Effet stabilisant du béton dans les éléments mixtes

Begrenzung des Beulens von Stahl durch den Beton im Verbundbau

Masami SAKAI
Dr. Eng.
Nippon Kokan K. K.
Kawasaki, Japan

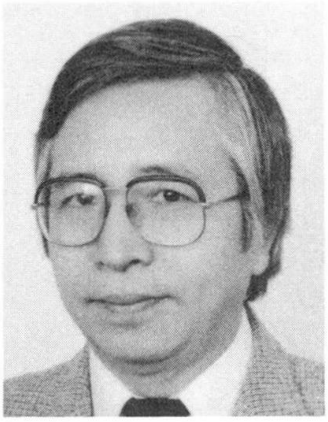

Masami Sakai, born 1938, did research on steel structures for a Master's degree of Yokohama National Univ. 1967, awarded Dr. of. Eng. by Tokyo Univ. 1985 and is now working on composite materials and structures.

Nobuhiko CHIDA
Structural Eng.
Nippon Kokan K. K.
Kawasaki, Japan

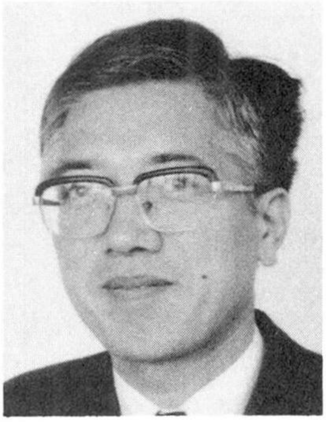

Nobuhiko Chida, born 1939, did research on differential settlement of foundations at Tohoku Univ. He designed steel structures for 19 years at N. K. K. and is now working on new materials for buildings.

Toshio NASU
Structural Eng.
Nippon Kokan, K. K.
Kawasaki, Japan

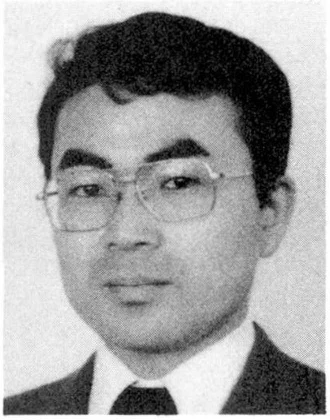

Toshio Nasu, born 1950, did research on cracking of concrete for a Master's degree of Osaka Univ. 1977, worked on the aseismic design of steel structures for 4 years at N. K. K., and is now working on steel and concrete composite structures.

SUMMARY

A steel plate element in a composite member of steel and concrete may be confined by concrete, hence it is possible to prevent the occurrence of local buckling even if the plate element has a large width-thickness ratio. In this study, experiments were first conducted on 76 specimens. Then, theoretical investigation was made by use of the Energy Method on the ductility of H steel flange. As a result, the effect of concrete on the ultimate strength, ductility and stiffness of composite members could be quantitatively determined.

RÉSUMÉ

Les éléments plans des profilés en H sont stabilisés au voilement par le béton, dans le cas de colonnes ou de poutres composites; il est possible de prévenir ce phénomène même pour des élancements (rapport largeur/épaisseur) élevés. On a tout d'abord expérimenté 76 éprouvettes pour étudier le voilement, la ductilité et la rigidité. Ensuite, sur ces critères, une étude théorique a été conduite, utilisant la méthode énergétique. Ainsi, les auteurs ont pu montrer l'effet stabilisant du béton.

ZUSAMMENFASSUNG

Ein Stahlplattenelement in einem Verbundbauteil aus Stahl und Beton kann durch den Beton gehalten werden, weshalb es möglich ist, dass das lokale Beulen des Plattenelementes verhindert wird, auch wenn das Breite- zu Dicke-Verhältnis gross ist. Im Rahmen dieser Studie wurden 76 Versuchskörper getestet. Anschliessend wurden theoretische Untersuchungen des Verformungsverhaltens von Flanschen bei H-Profilen mittels der Energie-Methode durchgeführt. Als Ergebnis konnte die Wirkung des Betons auf die Tragfähigkeit, Verformbarkeit und Steifigkeit von Verbundelementen quantitativ bestimmt werden.

1. OUTLINE OF EXPERIMENT

The experimental parameters are given in Table 1, the section types of specimen are shown in Fig.1 and the loading types in Fig.2.

2. RESULTS OF EXPERIMENT

2.1 Buckling mode of steel

The steel buckling mode of section type H-1 is shown in Fig.3(a). On the contrary, in the case of the section type H-3, the effect of inside concrete is shown in Fig.3(b). In the case of section type H-4, it is as shown in Fig.3(c). Accordingly, the stronger the confinement by concrete is, the smaller the buckling wave length is (Fig.4). Fig.5 shows the relation between the position of hoop reinforcement and the curvature

Table .1 Experimental parameters

Parameter	Level
B/t_f	9.5,10,15,20,23,30,33,48,62.5
Pw(%)	0, 0.1,0.2,0.4
tc(mm)	0, 20, 40, 64
N/No	0, 0.15, 0.3, 0.6, 1.0

B/t_f: Width-thickness ratio
Pw: Hoop reinforcement ratio
tc: Thickness of concrete cover
N/N_o: Compression ratio
No: Yield compression load of steel

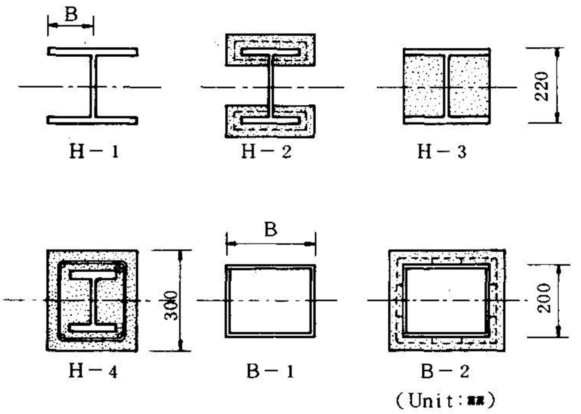

Fig.1 Section types of specimen

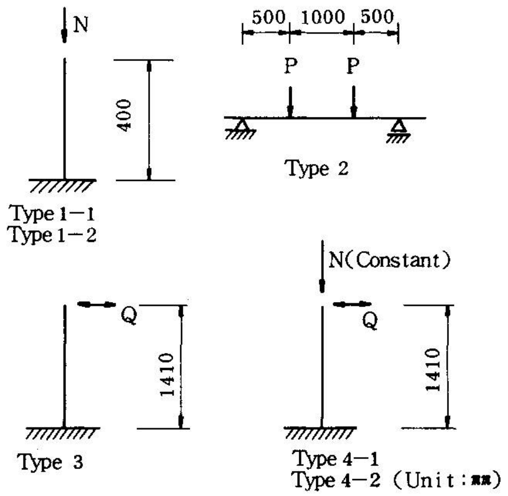

1-1, 4-1 Steel is only compressed
1-2, 4-2 Steel and concrete are compressed

Fig.2 Loading types

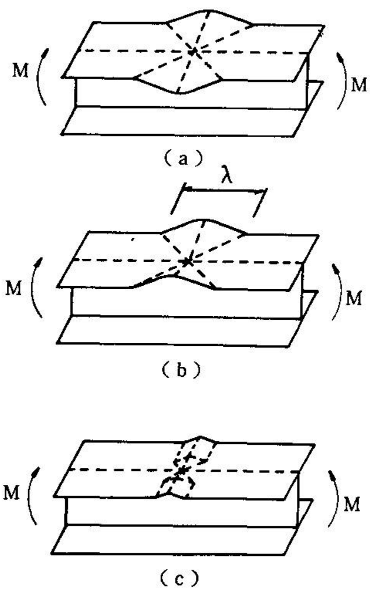

Fig.3 Buckling mode of steel

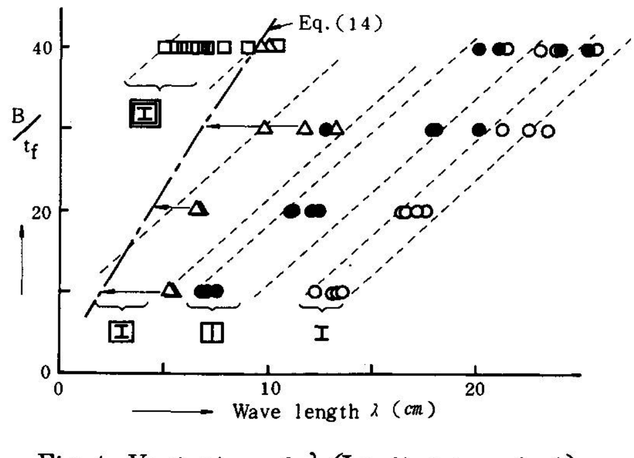

Fig.4 Variation of λ (Loading type 1-1)

distribution of steel flange obtained from test. As is clear from this figure, buckling of flange is under the influence of hoop reinforcement pitch. In this experiment, the buckling wave length was 1.5p on the average for the H-type.

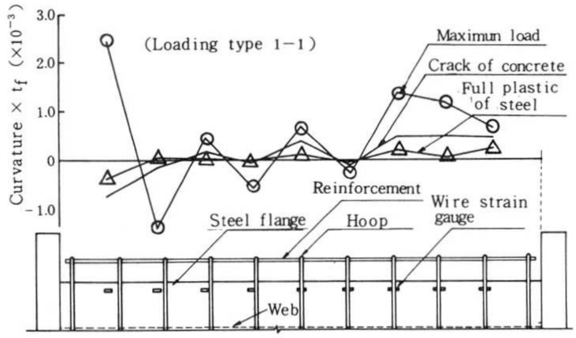

Fig.5 Deformation of steel flange (Pw=0.2%)

2.2 Failure mode of concrete cover

In the case of loading type 1-1 and section type H-4 bending crack(1) are observed in the center of concrete (Photo.1-(a)). This fact indicates that the steel flange will first push the central area of concrete cover. In the case of section type B-1, the wave corresponding to the flange and that corresponding to the web shift by half wave-length to each other. In the presence of confinement by concrete, however, both the shifting of wave-length and wave length itself become smaller.
In terms of loading type 1-2, the concrete cover is pushed-out due to local buckling of steel either prior to the collapse of concrete (Photo. 1-(b)) or after the collapse of concrete. The former was observed in case of no hoop reinforcement and the latter was observed in the case when the concrete was firmly confined by hoop reinforcement.

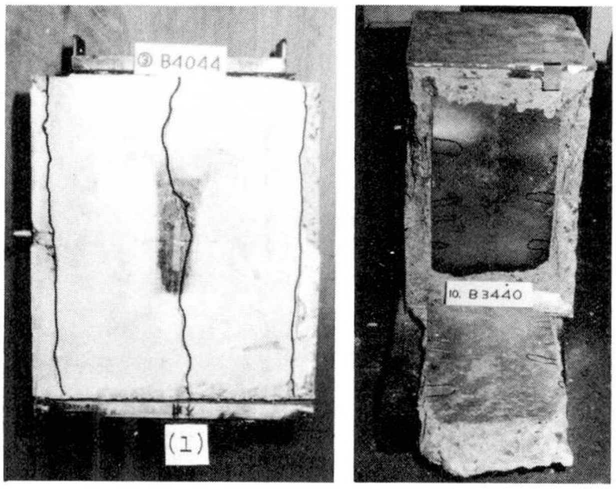

(a) Loading type 1 - 1 (b) Loading type 1 - 2

Photo.1 Failure mode of concrete cover

2.3 Failure of hoop reinforcement

Fig.6 shows the strain of hoop reinforcement of loading type 1-1. Step 1 is the value just after cracking, and Step 2 is the value just before collapse. The strain of point (4) is distinguished at the initial stage, but at the final stage, the strain

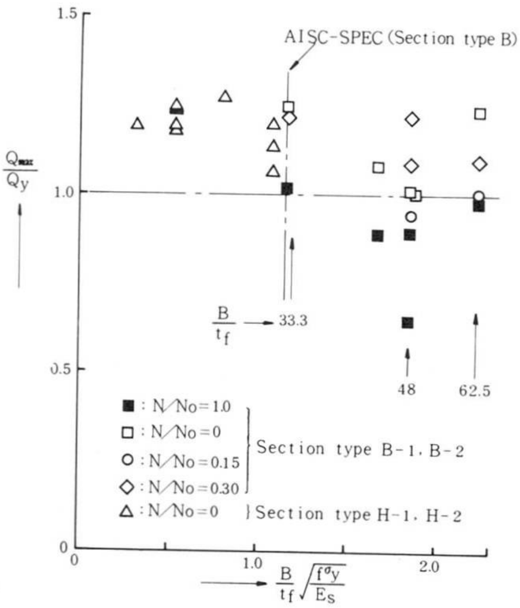

Fig.7 Maximum load and B/tf (Loading type 3, 4-1)

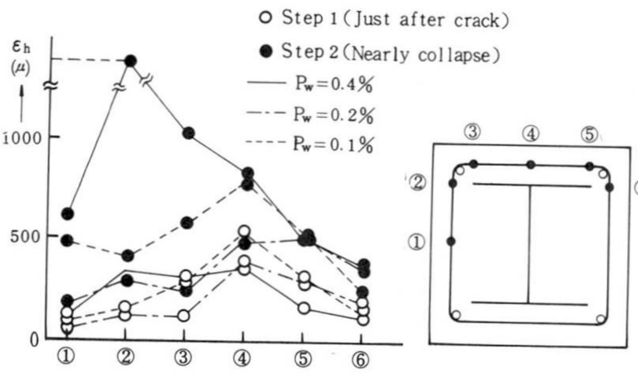

Fig.6 Strain of hoop reinforcement

on or around the flange end is sharply increasing toward the failure.

2.4 Ultimate strength of member

Fig.7 shows the ultimate strength of composite members obtained from the experiments of section type H-1,H-2,B-1,B-2 loading type 3,4-1. Even if the width-thickness has a ratio of B/tf = 62.5, it is possible to secure the full plastic strength of steel with the aid of the effect of confinement by concrete. However, the larger the compression ratio N/No is, the lower the ultimate strength is. Fig.8 shows the ultimate strength of section type H-1,H-3,H-4 loading type 1-1 paying close attention to the degree of confinement by concrete. By coating grease on the steel surface its bond with the concrete was broken. This figure indicates that as the degree of confinement by concrete increases, it approaches full plastic strength.

Fig.9 shows the data of loading type 4-2. Likewise in a situation when only the steel was compressed, the larger the width-thickness ratio B/tf and compression ratio are, the lower the ultimate strength is. With the aid of confinement by concrete, however, it is possible to secure the full plastic strength. Judging from these results, it has been proven that the confinement by concrete can improve the ultimate strength of steel. The Eq.(1) is the regression formula for determination of the ultimate strength of section type B-2 induced from the experiment.

$$\frac{M_{max}}{M_{the}} = \left(2.36-2.09\frac{N}{N_o}\right)\frac{t_c}{100t_f} + 9.04\times10^{-4}\left(\frac{B}{t_f}\right)^2 - 0.1\frac{B}{t_f} + 3.5 \quad ---(1)$$

where, Mmax: Maximun resisting moment of section
Mthe: Theoretical full plastic moment of steel

The Eq.(1), the full plastic moment (Theoretical 1) and the maximum moment on the assumption that all the section has been subjected to strain hardening (Theoretical 2) are compared in Fig.10.

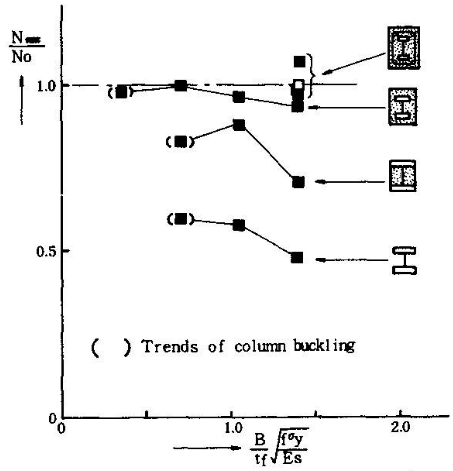

Fig.8 Maximum load and B/tf (Loading type 1-1)

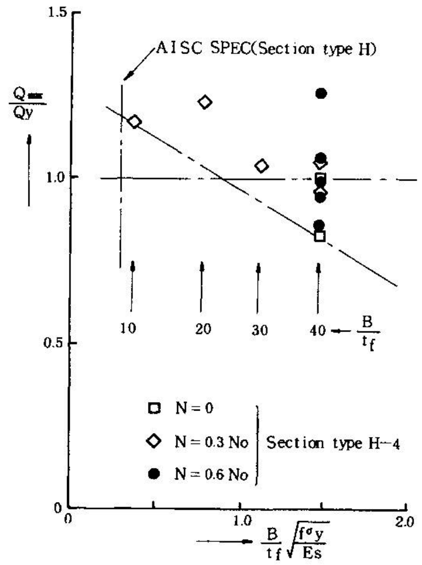

Fig.9 Maximum load and B/tf (Loading type 4-2)

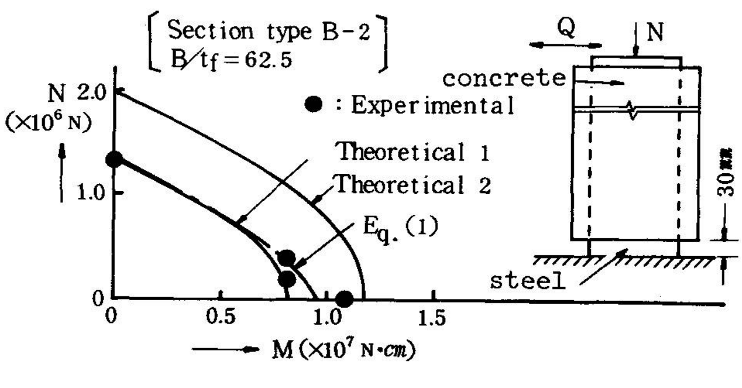

Fig.10 Maximum load (Loading type 4-1)

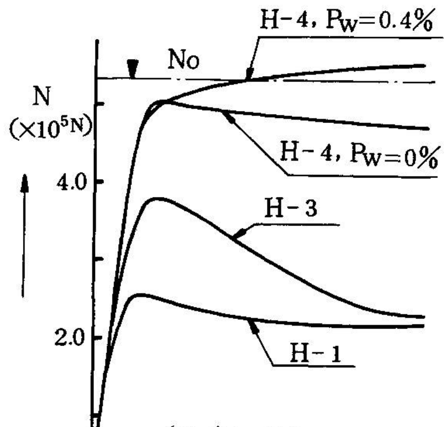

Fig.11 N-δ (Loading type 1-1)

2.5 Ductility of member

Fig.11 is the load-deformation curve of loading type 1-1. The steel surface have been greased. With the increase of flange confinement, ductility is improved. For the deformation at the ultimate strength, the effect of hoop reinforcement is particularly significant. Fig.12 shows the influence of flange width-thickness ratio in case of loading type 3. This figure indicates that, with the increase of width-thickness ratio, the ductility is lowered. However, if the hoop reinforcement is increased in volume, the ductility will be improved as is shown in Fig.13. It should be noted that, in the case when the similar experiment is conducted in loading type 4-2, the ductility may not be much improved. In this case the concrete cover is liable to separate from the inside concrete because of the small pitch of hoop reinforcement.

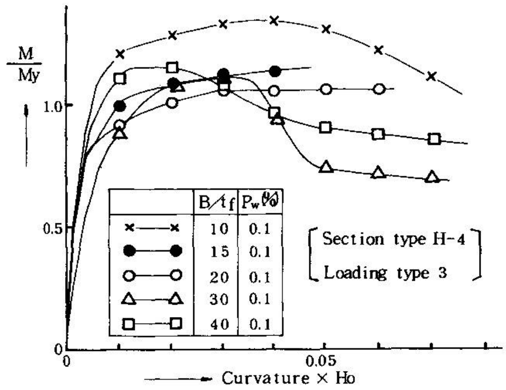

Fig.12 Moment-Curvature

2.6 Stiffness of member

Fig.14 shows the specimen's stiffness EI made dimensionless form by the theoretical stiffness of steel EsIs. It is clear from this figure that, with an increase in the compression ratio, the stiffness is higher. Then contribution rate of concrete for stiffness @ will be determined from the experimental values. For the section type B-2 and loading type 4-1, Eq.(2) is established.

$$\alpha = -0.0564 + (0.00462 + 0.0687\frac{N}{N_o})\frac{t_c}{t_f} \quad \text{---(2)}$$

provided that, when $\alpha < 0$, $\longrightarrow$ $\alpha = 0$

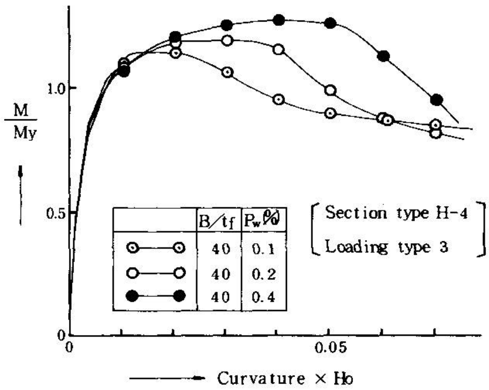

Fig.13 Moment-Curvature

3. DUCTILITY OF STEEL FLANGE PLATE

For the study of ductility in plastic region of steel plate, there is one method in which the stabilizing conditions for the plate are deduced using the plastic flow theory (Haaijer[3],etc.) and another one where they are deduced by the Energy Method based on the assumed buckling mode of the plate (Kato & Hukuchi[1]). In this study, theoretical investigation are made on the ductility of steel plate by the latter method which permits comparatively easy determination of the influence by each confining factors.

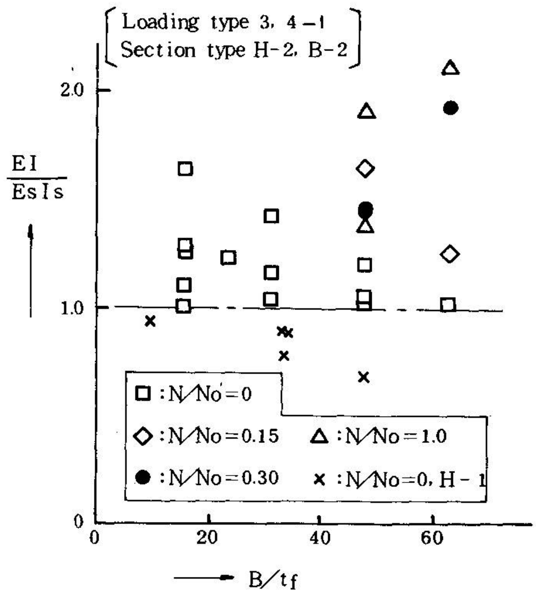

Fig.14 Stiffness of composite member

3.1 Assumptions for analysis

(1) The section type H-4 is to be investigated.

(2) Assuming that the bond between the steel and concrete is zero, the steel is only compressed.

(3) In the axial direction of each member, the web does not confine the flange deformation, but deforms together with the flange.

Based on these assumptions, the buckling and the failure modes of flange plate and concrete cover are defined and the volume of internal work nessesary for such deformation is expressed as a numerical formula. Then, from the experimental work equilibrium, the resisting moment per unit length in the hinge line of flange plate is determined. On the other hand the maximum possible moment per unit length in the hinge line is also deduced by using expanded Von Mises's yielding condition up to the strain hardening range. From these formulae the limit strain $_{s}\varepsilon_{max}$ of flange plate at the ultimate strength is deduced.

3.2 Defining of buckling mode

For steel flange plate it is assumed that plastic rotation takes place around the yield hinge line indicated in Fig.15, up to the ultimate strength of member. The pentagon $A_1A_2CA_4A_3$ is assumed to be contracted by δ from both sides into the pentagon $A_1'A_2'CA_4'A_3'$. At this time the triangles $A_2'CB_2'$, $A_4'CB_4'$, A_2A_4C and B_2B_4C are subject to shearing strain. The collapse mechanism of cover concrete is shown in Fig.16. As is also clear from Photo.1, the steel flange cannot be released from the confinement except for making cracks on the concrete cover along the line of flange end. Even in the case when there is no hoop reinforcement, it is considered that the comfinement of flange plate is effective if the concrete on both ends of flange is sound.

3.3 External work

The external work at the time when the flange plate deforms by 2δ under the yield compression load $2B\cdot t_f\cdot {}_f\sigma_y$ is

$$_{o}W = 4B\cdot t_f\cdot {}_f\sigma_y\cdot\delta \quad \text{---(3)}$$

3.4 Internal work

(1) The shearing strain work $_{i}W_{s1}$ of flange plates $A_2'CB_2'$ and $A_4'CB_4'$ is

$$_{i}W_{s1}=2\lambda\cdot t_f\cdot\delta\cdot\tau=2\lambda\cdot t_f\cdot\delta\cdot {}_f\sigma_y\cdot\sin\phi\cos\phi \quad \text{---(4)}$$

(2) The shearing strain work $_{i}W_{s2}$ of flange plates A_2CA_4 and B_2CB_4 is

$$_{i}W_{s2}=\lambda^2\cdot t_f\left(\frac{1}{\cos\theta}-1\right)\,{}_f\sigma_y\cdot\sin\phi\cos\phi \quad \text{---(5)}$$

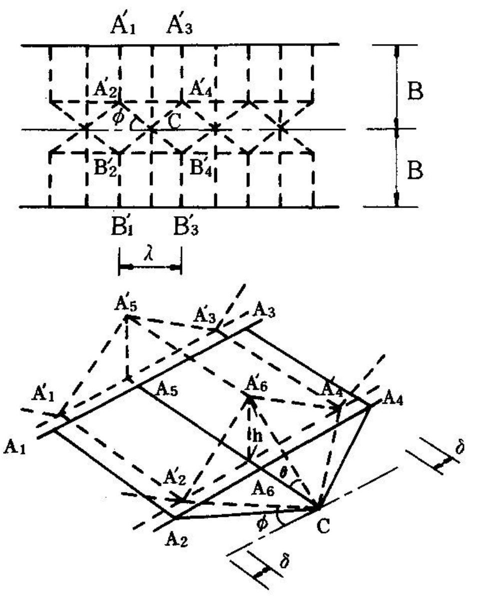

Fig.15 Buckling model of flange

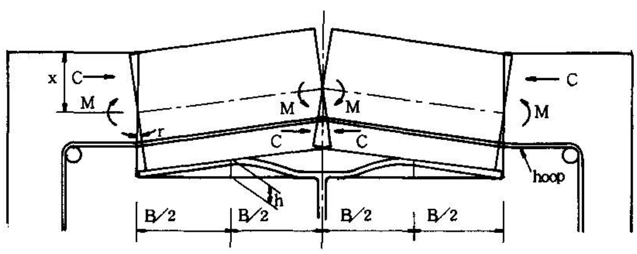

Fig.16 Collapse mechanism of concrete cover

(3) The work iWbs by rotation of flange plate hinge is

$$_iW_{bs} = \int_0^{\theta} (\Sigma M)\, d\theta \quad ----------------(6)$$

(4) The work iWbc by rotation of concrete cover's hinge is

$$_iW_{bc}=4M\theta = k_1k_3(1-k_2)\cdot Fc\cdot l_o\cdot\frac{\lambda}{B}\cdot tc^2\cdot\tan\theta \quad ---(7)$$

(5) The work of hoop reinforcement iWbh, using the elongation rate, is

$$_iW_{bh}={}_h\sigma_y\cdot P_w\cdot(B+d)\cdot l_o\cdot 2\{\sqrt{(2h)^2+B^2}-B\} \quad ----(8)$$

3.5 Equilibrium of work and limit strain

From the equilibrium of work, oW = iW, iWbs is determined as follows:

$$_iW_{bs}=K_1(1-\sqrt{1-\tan\theta})-K_2\left(\frac{1}{\cos\theta}-1\right)-K_3\tan\theta-K_4\left(\sqrt{\tan^2\theta+\left(\frac{B}{\lambda}\right)^2}-\frac{B}{\lambda}\right) \quad ---------(9)$$

$$\left.\begin{array}{ll} K_1=(4Bt_f\cdot {}_f\sigma_y-2\lambda t_f\tau)\frac{\lambda}{2} & K_2=\lambda^2 t_f\cdot\tau \\ K_3=k_1k_3(1-k_2)tc^2\cdot\lambda\cdot l_oFc/B & K_4=2\cdot{}_h\sigma_y\cdot Pw(B+d)\cdot\lambda\cdot l_o \end{array}\right\} \quad ------(10)$$

Therefore, the resisting moment M per unit length of hinge line determined from Eq.(6) with the total length of hinge line expressed as L is :

$$M=\frac{\Sigma M}{L}=\frac{1}{L}\cdot\frac{d({}_iW_{bs})}{d\theta}\fallingdotseq\frac{1}{L}\left(\sqrt{2\varepsilon}\cdot K_1-\sqrt{2\varepsilon}\cdot K_2-K_3-\frac{\lambda}{B}\sqrt{2\varepsilon}\cdot K_4\right) \quad ------------(11)$$

On the other hand, the maximum possible value of M is determined by expanding Von Mise's formula for strain hardening range in the same manner of Ref.[1] :

$$M=\frac{1}{4}{}_f\sigma_y t_f^2 m,\quad m=\frac{\beta^2-(2\sin^2\phi-\cos^2\phi)^2}{2\beta},\quad \beta=\sqrt{\cos^4\phi+4\left\{\left(\frac{{}_f\sigma_u}{{}_f\sigma_y}\right)^2-\cos^2\phi\,(1+2\sin^2\phi)\right\}} \quad --(12)$$

The limit strain of flange is derived from the Eq.(11) and Eq.(12). and expressed as Eq.(13) :

$$_s\varepsilon_{max}=\frac{\left(\frac{1}{4}\cdot{}_f\sigma_y\cdot m\cdot\bar{L}+\bar{K}_3\right)^2}{2(\bar{K}_1-\bar{K}_2-k\cdot\bar{K}_4)^2}\cdot\left(\frac{t_f}{B}\right)^2$$

$$= K\left(\frac{t_f}{B}\right)^2 \quad ---------- (13)$$

$$\bar{K}_1=2k\cdot{}_f\sigma_y-k^2\cdot\tau \qquad \bar{K}_2=2k^2\cdot\tau$$

$$\bar{K}_3=k_1k_3(1-k_2)\frac{l_o}{B}\left(\frac{tc}{t_f}\right)^2Fc\cdot k$$

$$\bar{K}_4=2\cdot{}_h\sigma_y\cdot l_oPw(B+d)k/(B\cdot t_f)$$

$$\bar{L}=\sqrt{2k}+3\ ,\quad k=\lambda/B$$

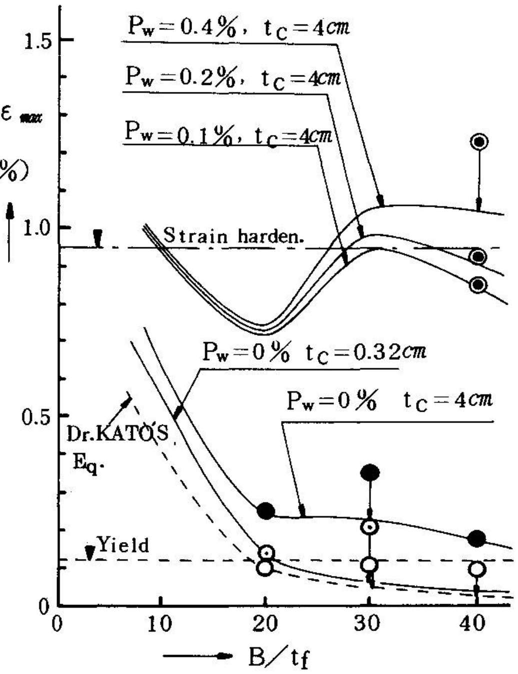

Fig.17 Limit strain of steel flange (Loading type 1-1, section type H-1, H-3, H-4)

Moreover, the buckling length of flange is expressed by Eq.(14) by partially differentiating the value of K in Eq.(13) by λ

$$\lambda = F\left(\frac{{}_f\sigma_u}{{}_f\sigma_y},\ \frac{tc}{t_f},\ Pw\ ,\ d\ \right) \quad ---(14)$$

The theoretical value of λ determined for the section type H-4 from Eq.(14) is shown in Fig.4. The value of ${}_s\varepsilon_{max}$ determined by substituting Eq.(14) in Eq.(13) using the width-thickness ratio B/tf as a parameter is shown in Fig.17. Judging from Fig.17, it seems that the larger the width-thickness ratio B/tf is the greater effect the concrete cover and hoop reinforcement have.

4. CONCLUSION

The findings of this study are as follows:

1) The buckling mode of steel flange varies greatly with the presence of concrete. In particular the buckling wave length of flange was significantly smaller due to the effect of confinement of concrete.

2)To secure the theoretical yield strength of composite members, the width-thickness ratio of steel flanges could be increased up to 40(H type) and 62.5(B type) through proper choice of concrete cover.

3) The ductility of composite members was significantly improved by the concrete cover. Especially the use of sufficient volume of hoop reinforcement is very effective to the ductility properties.

4) The limit strain of steel flange under the confinement of concrete was evaluated with various parameters using the Energy Method. And simulation of experimental values could be attained to a certain degree.

Notation

B: Half width of flange
t_f: Flange thickness
tw: Web thickness
tc: Concrete cover thickness
H: Height of steel section
Ho: Height of specimen's section
λ: Buckling wave length
p: Pitch of hoop reinforcement
Pw: Hoop reinforcement ratio
N/N_o: Compression ratio
C: Compressive force of concrete
k_1, k_2, k_3: $k_1 \cdot k_3 = 0.83, k_2 = o.42$
θ : Angle of flange plate rotation
γ: Angle of concrete cover rotation
ϕ : Angle of external force with flange hinge line
Mmax: Maximum resisting moment of section
lo: Effective length of concrete cover contributing to the confinement

d: (Beam width-2B)/2
δ: Deformation of flange
τ: Shearing Stress $(= {}_f\sigma_y \cdot \sin\phi \cos\phi)$
Fc: Compressive strength of concrete
Es: Elastic modulous of flange
ε: Strain of flange
${}_h\sigma_y$: Yield stress of hoop
${}_f\sigma_y$: Yield stress of flange
${}_f\sigma_u$: Ultimate stress of flange
${}_oW$: External work
${}_iW$: Internal work
α: Contribution rate of stiffness (El/Esls-1)

References:

(1) B.Kato & Y.Hukuchi "Flange local buckling in plastic range"(in Japanese), TRANSACTIONS of AIJ May,1968
(2) M.G.Lay "Flange Local Buckling in Wide Flange Shapes",ASCE,December,1965
(3) G.Haaijer "Plate Buckling in the Strain Hardening Range",ASCE,TRANSACTIONS paper,No.2968,1958
(4) M.Kimura "The Stiffening Effect for Local Buckling of High Strength Steel by Mortar"(in Japanese),Research Reports of AIJ Kanto Branch,1976